Multi-band circular polarizer based on a twisted triple split-ring resonator*

Wu Song(吴 松)[a)b)], Huang Xiao-Jun(黄晓俊)[a)c)], Xiao Bo-Xun(肖柏勋)[d)], Jin Yan(金 彦)[b)], and Yang He-Lin(杨河林)[a)†]

[a)] College of Physical Science and Technology, Central China Normal University, Wuhan 430079, China

[b)] Wuhan Engineering Science and Technology Institute, Wuhan 430019, China

[c)] Department of Physics, Kashgar Teachers College, Kashgar 844000, China

[d)] Engineering Geophysical Research Center, Yangtze University, Jingzhou 434023, China

(Received 6 June 2014; revised manuscript received 11 August 2014; published online 10 October 2014)

A multi-band circular polarizer using a twisted triple split-ring resonator (TSRR) is presented and studied numerically and experimentally. At four distinct resonant frequencies, the incident linearly polarized wave can be transformed into left/right-handed circularly polarized waves. Numerical simulation results show that a *y*-polarized wave can be converted into a right-handed circularly polarized wave at 5.738 GHz and 9.218 GHz, while a left-handed circularly polarized wave is produced at 7.292 GHz and 10.118 GHz. The experimental results are in agreement with the numerical results. The surface current distributions are investigated to illustrate the polarization transformation mechanism. Furthermore, the influences of the structure parameters of the circular polarizer on transmission spectra are discussed as well.

Keywords: multi-band, circular polarizer, chiral metamaterial

PACS: 78.67.Pt, 41.20.Jb, 42.25.Ja **DOI:** 10.1088/1674-1056/23/12/127805

1. Introduction

Metamaterials (MMs) are a new class of artificial composite materials consisting of periodically arranged dielectric cells and structured metallic elements. Over the past few decades, electromagnetic (EM) MMs have aroused the great interest of researchers, since special EM properties exist in MMs.[1–4] Based on MMs, arbitrary values of effective permittivity and permeability can be designed so that we have a good possibility of achieving some amazing applications including perfect lens.[5] Recently, a new class of chiral metamaterial (CMM) has been proposed and investigated widely due to its peculiar characteristics, e.g. circular dichroism,[6] optical activity,[7] negative index,[8] and asymmetric transmission.[9] Due to the lack of mirror symmetry, the cross coupling between the electric and magnetic fields exists in the CMM, which is the cause of these peculiar properties and can lead to the difference in the transmission coefficient between right-handed circularly polarized (RCP) and left-handed circularly polarized (LCP) waves, the CMM has the ability to manipulate the polarization state of the EM wave.[10–14] Many CMM structures have been reported to manipulate the polarization state of the EM wave for obtaining polarization transformation.[15–19] For example, the structure of twisted four U-shaped split ring resonators has been designed to convert incident linearly polarized waves into circularly polarized waves, with different directions of rotation at two distinct resonances.[18] Ye and He proposed a 90° polarization rotator using a bilayered chiral metamaterial with giant optical activity.[20] Li *et al*. presented broadband terahertz circular polarizers with single-and double-helical array metamaterials.[21] Zhao *et al*. proposed twisted optical metamaterials for planarized ultrathin broadband circular polarizers.[22] In general, there are two types of CMMs as a polarization transformer: a two-dimensional (2D) structure and a three-dimensional (3D) structure.[23,24] Compared with the 3D structure, the 2D structure is easy to fabricate and integrate into other small devices, such as electrical small antennas.[25]

In this paper, a 2D CMM structure on the basis of a twisted triple split-ring resonator (TSRR) is proposed as a circular polarizer. When a linearly polarized wave is incident on the designed structure, left-handed and right-handed circularly polarized waves can be obtained at four distinct resonances. Compared with other kinds of CMM circular polarizers,[26,27] the unit cell of the structure is extremely small in all three dimensions and the proposed circular polarizer has more resonant frequencies. Moreover, the proposed planar CMM has only one dielectric layer and is easily fabricated with conventional printed circuit board technology.

*Project supported by the National Natural Science Foundation of China (Grant No. 41474117) and the Special Funds for Development Scientific Research Unit Projects of Wuhan, China (Grant No. 2013BJ004).

†Corresponding author. E-mail: emyang@mail.ccnu.edu.cn

© 2014 Chinese Physical Society and IOP Publishing Ltd

2. Simulation, experiment, and results

Figure 1(a) shows the unit cell of the proposed structure. Each cell is composed of a pair of TSRRs. The TSRRs on the top layer and at the bottom layer are coaxial but mutually twisted by 90°. Due to the lack of C_4 symmetry in this CMM, the response to the incident electric field along the x direction is different from the y direction. In this design, circular polarization can be obtained only in the case of the y-polarization incident wave. Here we employ Rogers RO4003 as the dielectric lamina with a relative permittivity of 3.38 and a tangent loss of 0.0027. The metallic layers on both sides are both modeled as a 0.03-mm thick copper film. The period of the whole unit cell is p and its thickness is t and the optimized geometrical parameters are as follows: $p = 5$ mm, $t = 0.813$ mm, $w_1 = 0.2$ mm, $w_2 = w_3 = 0.4$ mm, $d = 0.6$ mm, $g = 0.2$ mm, $L_1 = 0.4$ mm, $L_2 = L_3 = 0.5$ mm, $r_1 = 1.6$ mm, $r_2 = 1.0$ mm, and $\theta = 120°$.

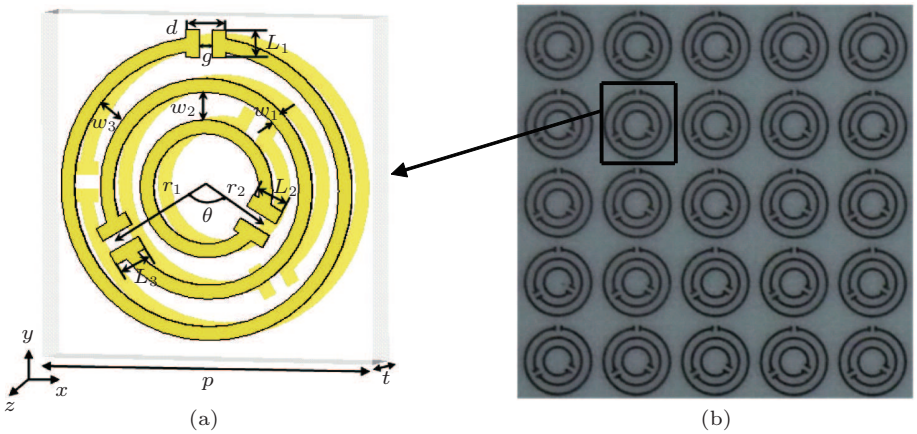


Fig. 1. (color online) (a) Unit cell of circular polarizer. (b) Part of the photo of the experimental sample.

Numerical simulation is performed to demonstrate the characteristics of the CMM by using CST Microwave Studio 2012. A broadband y-polarized wave propagating in the $-z$ direction is used as an excitation source in the simulation. The boundaries are selected to be periodic in the x and y directions and open in the $z$direction. In the experiment, we fabricate the CMM sample with a size of 36×36 unit cells, and part of the photo of the experimental sample is shown in Fig. 1(b). A linearly polarized horn antenna is employed as a transmitter while an LCP or an RCP antenna is utilized as a receiver in turn. The antennas are connected to two ports of a vector network analyzer of Agilent PNA E8362B. The prototype is placed in the middle between the antennas.

Simulated and experimental linear-circular transmission coefficients $T_{\pm y}$ are depicted in Fig. 2(a), where the subscript '+' indicates the RCP wave and the subscript '−' refers to the LCP wave. The second subscript 'y' indicates the incident field polarization (y-polarized). For a circular polarizer, the goal is that one circularly polarized wave is much larger (smaller) than the other one, i.e. $T_{+y} \gg T_{-y}$ or $T_{+y} \ll T_{-y}$. The simulated results show that there are, obviously, four transmission dips in the frequency band ranging from 5.5 GHz to 11 GHz. The dip values of the RCP waves are −29 dB and −22.2 dB at 7.292 GHz and 10.118 GHz respectively, while the transmissions of the LCP wave are −2.54 dB and −3.25 dB. The dip values of the LCP waves are observed at 5.738 GHz to be −35 dB and at 9.218 GHz to be −30.8 dB, while the transmissions of the RCP waves are −2.97 dB and −2.48 dB. It follows from the feature of the circular polarizer that the studied CMM originates from the different circular polarization transmissions for RCP and LCP components, due to a y-polarized incident. One of the circular polarizations is eliminated at the resonant frequencies, whereas the other polarization is transmitted with a small loss. As a result, the transmitted wave is RCP at 5.738 GHz and 9.218 GHz. Similarly, at 7.292 GHz and 10.118 GHz, the LCP wave is transmitted. Furthermore, the ratio between the amplitudes of the two circularly polarized transmission waves are shown in Fig. 2(b). We can observe that the difference between the transmitted waves with different circular polarizations can reach a level of more than 20 dB. These results further confirm that circularly polarized waves with different rotation angles are realized at the four frequencies. The RCP waves are produced at 5.738 GHz and 9.218 GHz, and the LCP waves are obtained at 7.292 GHz and 10.118 GHz. According to the experimental results (see Figs. 2(a) and 2(b)), we can see that the RCP waves are produced at 6.114 GHz and 9.429 GHz, and LCP waves are produced at 7.550 GHz and 10.355 GHz. The four resonant frequencies as a whole shift towards a higher frequency by about 0.3 GHz, which is mainly attributed to the fabrication tolerance and measurement error. The size and the relative permittivity of the CMM sample can affect the resonant frequencies. If the size and the relative permittivity of the CMM sample is smaller than the real values, the resonant frequencies will shift towards the higher frequencies.

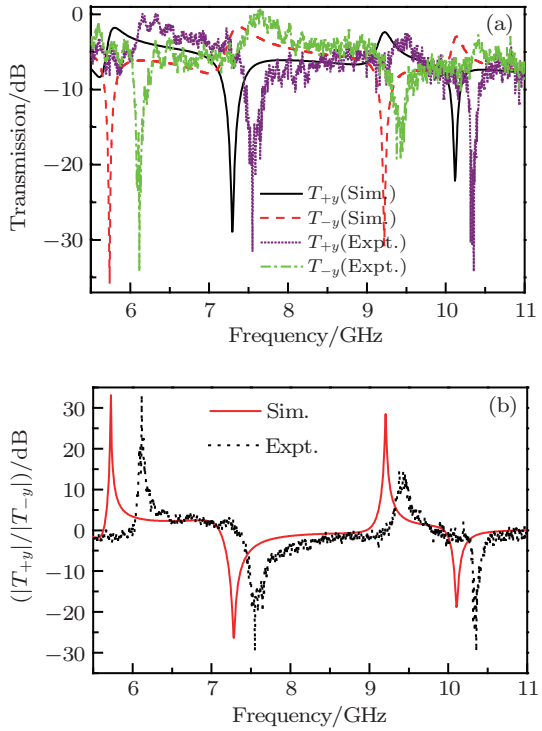


Fig. 2. (color online) Simulated and experimental results for (a) the linear-circular transmission coefficients, and (b) the difference between the transmitted RCP and LCP waves.

In order to demonstrate the polarization characteristics of the transmitted wave, the ratio of the cross-polarization transmission to co-polarization transmission $|T_{xy}|/|T_{yy}|$ is also calculated, and the corresponding result is depicted in Fig. 3 which also includes the value of the phase difference $\Phi(T_{xy}) - \Phi(T_{yy})$ at the frequency band. It can be seen that the values of $|T_{xy}|/|T_{yy}|$ are 0.96, 1.09, 1.08, and 1.24 at 5.738 GHz, 7.292 GHz, 9.218 GHz, and 10.118 GHz, respectively. The corresponding phase differences are equal to 90.49°, −91.72°, 89.48°, and −93.40°, respectively. The calculated results indicate that the RCP waves are realized at 5.738 GHz and 9.218 GHz for an incident y-polarized wave along the $-z$ direction, while LCP waves are produced at 7.292 GHz and 10.118 GHz. Meanwhile, the results are in good agreement with the results of the circular polarization transmission in Fig. 2(a).

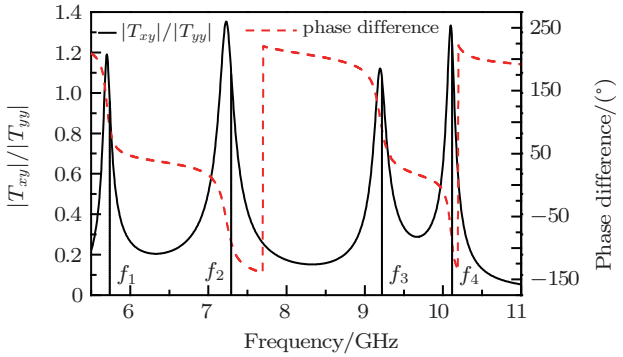


Fig. 3. (color online) Ratio of $|T_{xy}|/|T_{yy}|$, and phase difference of $\Phi(T_{xy}) - \Phi(T_{yy})$.

The polarization azimuth rotation angle θ and ellipticity η of the proposed CMM are calculated by the following formulas for the incident y-polarized wave as[13,24]

$$\theta = \frac{1}{2}[\arg(T_{+y}) - \arg(T_{-y})], \tag{1}$$

$$\eta_y = \frac{1}{2}\sin^{-1}\left\{\frac{|T_{+y}|^2 - |T_{-y}|^2}{|T_{+y}|^2 + |T_{-y}|^2}\right\}, \tag{2}$$

where the transmissions of circularly polarized waves $T_{\pm y}$ can be converted from the linear transmission coefficients into cross-polarization T_{xy} and co-polarization T_{yy}, and $T_{\pm y} = (T_{xy} \pm \mathrm{i}T_{yy})/\sqrt{2}$. The polarization azimuth rotation angle θ denotes the rotation angle between the polarization planes of the transmitted and incident waves, and the ellipticity η describes the polarization state of the emitted wave. For a purely circularly polarized wave, η equals ±45°. For a purely linearly polarized wave, $\eta = 0°$ and the polarization plane has a rotation angle of θ with respect to the incident wave. When η is larger than zero, the emitted wave is right-handed, otherwise it is left-handed. The calculated results of θ and η_y for the incident y-polarized wave are shown in Figs. 4(a) and 4(b), respectively. It can be clearly seen that the value of η_y are 43.70°at 5.738 GHz, −42.28° at 7.292 GHz, 42.80° at 9.218 GHz, and −38.59° at 10.118 GHz, which means that the transmitted waves are close to pure circular polarization. Furthermore, it can be also found that the values of ellipticity η_y equal about 0° at 5.644 GHz, 7.105 GHz, 8.993 GHz, and 9.944 GHz, respectively, where the linearly polarized waves are produced. The values of the corresponding polarization azimuth rotation angle θ are 35.5°, −38.4°, 21.3°, and −25.5°, respectively, which means the giant optical activity effect and the polarization planes of the emitted wave have 35.5°, −38.4°, 21.3°, and −25.5° rotation angles with respect to the incident wave, respectively.

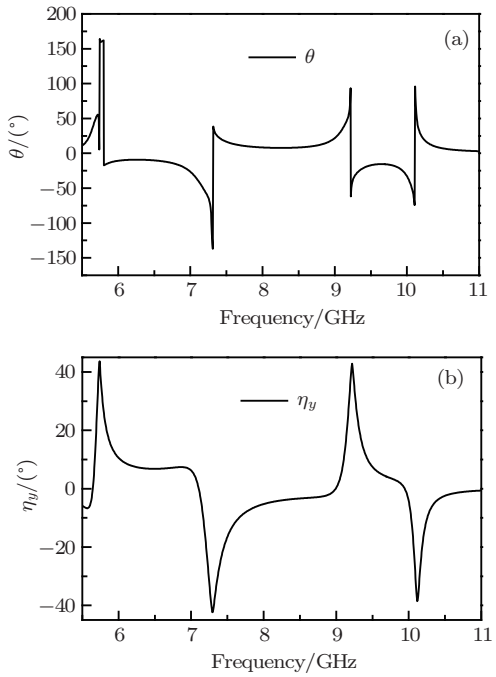


Fig. 4. Simulated results for (a) polarization azimuth rotation θ and (b) ellipticity versus frequency.

3. Discussion

In order to better understand the physical origin of the linear-circular polarization transformation, the surface current distributions at the four resonant frequencies are calculated and studied as shown in Fig. 5. From Figs. 5(a) and 5(c), we can see that the currents on the top and at the bottom TSRRs are in the same direction at 5.738 GHz and 9.218 GHz, which exhibits a symmetric resonance mode as coupled electric dipoles resonance.[28] This results in equalizing the orthogonal components of the electric field with about 90°-phase difference at the output interface.[28]

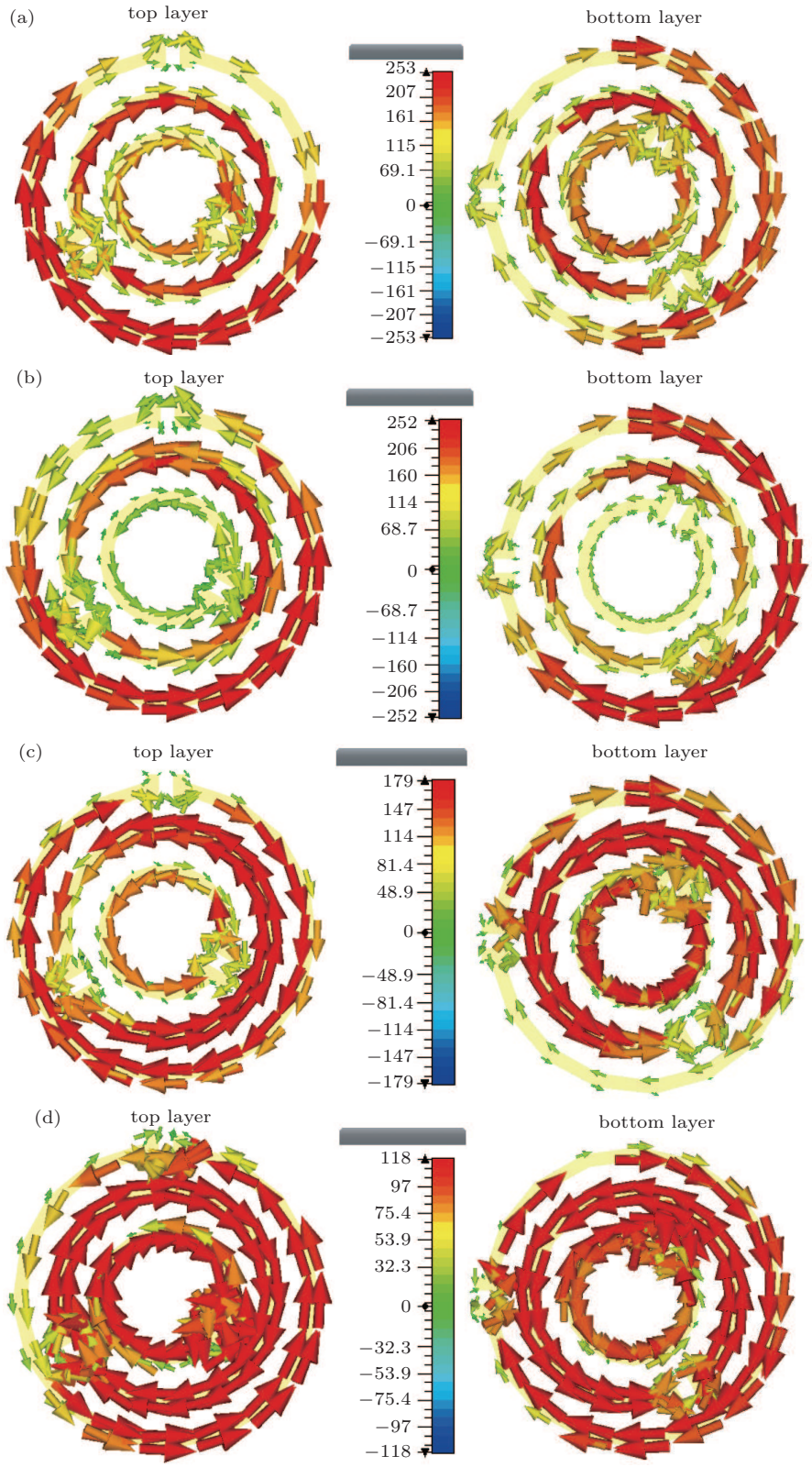


Fig. 5. (color online) Surface current distributions at (a) 5.738 GHz, (b) 7.292 GHz, (c) 9.218 GHz, and (d) 10.118 GHz.

Therefore, the transmitted waves are RCP waves at 5.738 GHz and 9.218 GHz. As shown in Figs. 5(b) and 5(d), the directions of the surface currents on the top layer and at the bottom layer are opposite at 7.292 GHz and 10.118 GHz, which corresponds to an asymmetric resonance mode as coupled magnetic dipole resonance. This results in equalizing the orthogonal components of the electric field with about $-90°$-phase difference. Thus, the transmitted waves become LCP waves. We can also observe that the current on the outer split-ring resonator (SRR) is much stronger than the currents on the other SRRs at 5.738 GHz and 7.292 GHz, so the polarization transformations at these two resonant frequencies are mainly attributed to the outer SRR. The current flowing in the middle SRR is very strong and the current flowing in the inner SRR is not very weak at 9.218 GHz nor 10.118 GHz, and the polarization transformation at these two resonant frequencies are related to the middle SRR and inner SRR. The middle SRR has a larger effect on the polarization transformation at 9.218 GHz and 10.118 GHz, while the inner SRR has a smaller effect on the polarization transformation at these resonant frequencies. Although the inner SRR has a smaller effect on the polarization transformation, it is necessary to retain the inner SRR in the proposed structure for obtaining polarization transformations at 9.218 GHz and 10.118 GHz.

In order to study the influences of the structure parameters on the transmission spectra, the analysis of the parameter is carried out by varying certain parameters while keeping the other parameters fixed. Figures 6(a) and 6(b) present the transmission coefficient spectra for RCP and LCP waves with different values of L_1, L_2, and L_3. We can see that the positions of frequencies for RCP and LCP waves both shift towards higher frequencies as the values of L_1, L_2, and L_3 increase. It can be noted that the difference between the transmitted waves with different circular polarizations obviously increases at the first resonant frequency as the values of L_1, L_2, and L_3 increase, while at the other three resonant frequencies, the difference between the transmitted waves with different circular polarizations almost remains the same by increasing the values of L_1, L_2, and L_3. So the values of L_1, L_2, and L_3 have large influences on the first resonant frequency.

Figure 7 shows the transmission spectra when the gap g varies from 0.1 mm to 0.3 mm. The resonant positions shift towards the higher frequencies as g increases. We can see that the difference between the transmitted waves with different circular polarizations obviously increases at the first resonant frequency as g increases, while the difference between the transmitted waves with different circular polarizations decreases slightly at other resonant frequencies as g increases. Therefore, parameter g has an influence on the four resonant frequencies. According to the analysis results, we can adjust the values of L_1, L_2, and L_3, and parameter g to manipulate the resonant frequencies and obtain the circularly polarized wave that is close to a purely circularly polarized wave. The mechanism of frequency shift is easy to understand based on the *L*–*C* resonance circuit theory. The split in the proposed structure is similar to a capacitor. According to *L*–*C* resonance circuit theory, the resonance frequency is calculated

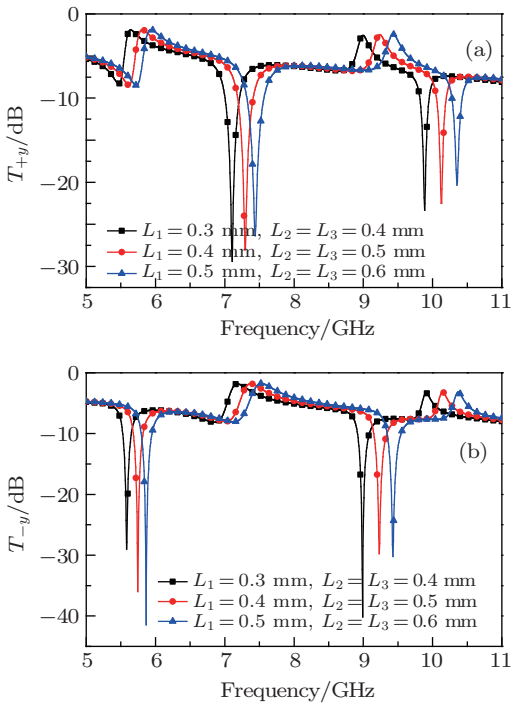


Fig. 6. (color online) Transmission spectra for different lengths (L_1, $L_2 = L_3$), (a) transmission of RCP wave, (b) transmission of LCP wave versus frequency.

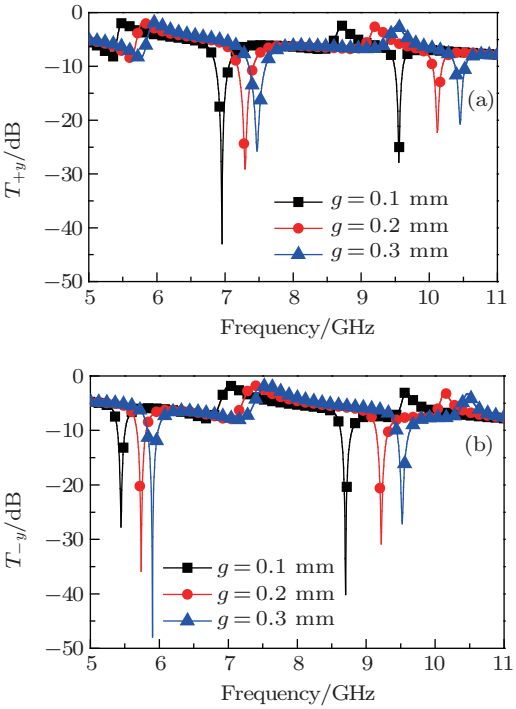


Fig. 7. (color online) Transmission spectra for different values of gap g, (a) transmission of RCP wave, (b) transmission of LCP wave versus frequency.

from $\omega = 1/\sqrt{LC}$ where L is the total inductance and C is total capacitance. By increasing the values of g, L_1, L_2, and L_3, C will decrease, finally resulting in the increase of resonance frequency.[29]

4. Conclusion

In this paper, we propose a multi-band asymmetric CMM based on the structures of bi-layer twisted TSRR. Both simulation and experimental results have proved that the circular polarization waves are obtained at four frequencies, when the structure is illustrated by a y-polarized wave propagating in the $-z$ direction. The design can be used as a circular polarization transformer for microwave applications. The major advantages of the structure are that they are electrically thin and easy to fabricate. Furthermore, the proposed CMM could be developed to explore more potential applications in circularly polarized antenna systems.

References

[1] Shelby R A, Smith D R and Schultz S 2001 *Science* **292** 77
[2] Smith D R, Padilla W J, Vier D C, Nemat-Nasser S C and Schultz S 2000 *Phys. Rev. Lett.* **84** 4184
[3] He Q, Sun S L, Xiao S Y, Li X, Song Z Y, Sun W J and Zhou L 2014 *Chin. Phys. B* **23** 047808
[4] Mo M M, Wen Q Y, Chen Z, Yang Q H, Qiu D H, Li S, Jing Y L and Zhang H W 2014 *Chin. Phys. B* **23** 047803
[5] Pendry J B 2000 *Phys. Rev. Lett.* **85** 3966
[6] Decker M, Klein M W, Wegener M and Linden S 2007 *Opt. Lett.* **32** 856
[7] Plum E, Fedotov V A and Zheludev N I 2008 *Appl. Phys. Lett.* **93** 191911
[8] Plum E, Zhou J, Dong J, Fedotov V A, Koschny T, Soukoulis C M and Zheludev N I 2009 *Phys. Rev. B* **79** 035407
[9] Mutlu M, Akosman A E, Serebryannikov A E and Ozbay E 2011 *Opt. Express* **19** 14290
[10] Ye Y and He S 2010 *Appl. Phys. Lett.* **96** 203501
[11] Xie L Y, Yang H L, Huang X J and Li Z J 2013 *Prog. Electromagn. Res.* **141** 645
[12] Ma X L, Huang C, Pu M, Wang Y Q, Zhao Z Y, Wang C T and Luo X G 2012 *Appl. Phys. Lett.* **101** 161901
[13] Cheng Z Z, Cheng Y Z and Fang C H 2014 *J. Electromagn. Waves Appl.* **28** 485
[14] Li S, Li J Q and Cao Y S 2013 *Chin. Phys. B* **22** 117806
[15] Li Z, Zhao R, Koschny T, Kafesaki M, Alici K B, Colak E, Caglayan H, Ozbay E and Soukoulis C M 2010 *Appl. Phys. Lett.* **97** 081901
[16] Zhang S, Park Y S, Li J, Lu X, Zhang W and Zhang X 2009 *Phys. Rev. Lett.* **102** 023901
[17] Zhou J, Dong J, Wang B, Koschny T, Kafesaki M and Soukoulis C M 2009 *Phys. Rev. B* **79** 121104
[18] Mutlu M, Akosman A E, Serebryannikov A E and Ozbay E 2011 *Opt. Lett.* **36** 1653
[19] Zheludev N I, Plum E and Fedotov V A 2011 *Appl. Phys. Lett.* **99** 171915
[20] Ye Y Q and He S L 2010 *Appl. Phys. Lett.* **96** 203501
[21] Li S X, Yang Z Y, Wang J and Zhao M 2011 *J. Opt. Soc. Am. A* **28** 19
[22] Zhao Y, Belkin M A and Alu A 2012 *Nat. Commun.* **3** 870
[23] Yang Z Y, Zhao M, Xie P X, Wu L, Lu Z Q and Zhang P 2012 *IEEE Photon. Technol. Lett.* **24** 1708
[24] Yan S and Vandenbosch G A E 2013 *Appl. Phys. Lett.* **102** 103503
[25] Ziolkowski R W and Erentok A 2006 *IEEE Trans. Anten. Propag.* **54** 2113
[26] Ye Y Q, Li X, Zhuang F and Chang S W 2011 *Appl. Phys. Lett.* **99** 031111
[27] Zhu W R, Rukhlenko I D, Xiao F J and Premaratne M 2014 *J. Appl. Phys.* **115** 143101
[28] Cheng Y Z, Nie Y, Wang X and Gong R Z 2013 *Appl. Phys. A* **111** 209
[29] Li M H, Liu S Y, Guo L Y, Lin H, Yang H L and Xiao B X 2013 *Opt. Commun.* **295** 262